Phase ordering in the Ising model with conserved spin

J.F. Marko
Center for Studies in Physics and Biology, The Rockefeller University, 1230 York Avenue, New York, New York 10021-6399

G.T. Barkema
Laboratory of Atomic and Solid State Physics, Clark Hall, Cornell University, Ithaca, New York 14853-2501
(Received 27 February 1995)

We have studied conserved-order-parameter domain growth following a quench from $T = \infty$ to $T < T_c$ at critical concentration in the two- and three-dimensional Ising model, using a type of magnetization-conserving spin-exchange dynamics which suppresses diffusion along interfaces. Domain sizes grow in proportion to the $\frac{1}{3}$ power of time after the quench over a wide range of annealing temperatures. The effective diffusion constant associated with the growth law is thermally activated, leading to a long lag time $\sim \exp(\text{const}/T)$ before the onset of power-law growth. During this lag period, transient phenomena associated with activated barrier crossings are observed. We also study dynamic scaling of the structure factor and two-time correlations in the asympototic growth regime: many of these results differ from those obtained from continuous-field theories of phase separation such as model B.

PACS number(s): 05.70.Ln, 64.75.+g, 64.60.Ht

I. INTRODUCTION

Binary mixtures undergo phase separation via formation and growth of bubbles, or domains, of the two coexisting phases. In many cases, the characteristic domain size grows according to a power law of time. The kinetics of demixing have been studied extensively for binary alloys [1], liquid mixtures [2], and polymer blends [3]. In cases where hydrodynamic flows [4] and other nondiffusive transport processes may be ignored, these coarsening processes may be modeled using dynamical Ising models with locally conserved magnetization. The two values that may be taken by each spin represent the two species of particles that are demixing. The coarse-grained magnetization of such models is generally believed to be described by a Langevin equation (so-called model B) [5]. If one phase occupies a small volume fraction, in which case the minority phase is organized into spherical bubbles, the theory of Lifshitz, Slyozov, and Wagner (LSW) [6] suggests that the average domain size asymptotically increases as $R \sim t^n$ with $n = 1/3$.

Simple scaling arguments suggest that the LSW growth law holds for arbitrary volume fractions and in all space dimensions [7]. Consider the asymptotic growth regime where the domain size R is much larger than any other lengths such as the domain wall thickness and the size of the constituent particles. If the surface tension between the two types of domains is σ then the excess free energy (the remaining free energy stored in the domain walls) per volume is on the order of σ/R for any dimension d. As this excess free energy will be inhomogeneous on the scale R we expect chemical potential gradients on the order of σ/R^2. These gradients give rise to forces on the constituent particles, driving a current on the order of $M\sigma/R^2$ where M is a transport coefficient. This current is the volume of one phase transported across a unit $(d-1)$-dimensional area of interface per unit time, and is thus on the order of the domain wall velocity dR/dt. Therefore $dR/dt \sim R^{-2}$ or $R \sim t^{1/3}$.

Beyond scaling arguments of this sort, there is no reliable analytical theory of phase separation, and most of what is known comes from large-scale computer simulations. The LSW growth law described above has been observed in simulations of model B in two [8–10] and three dimensions [11], and the two-dimensional square-lattice Ising model with locally conserved magnetization [7,12,13] for various volume fractions.

Here we expand a previously published report [14] of the first observation of the LSW growth law for a three-dimensional (3D) dynamical Ising model at critical concentration. We should have emphasized in our earlier paper that the pioneering study of Marro, Lebowitz, and Kalos [15] observed a growth exponent $n = 1/3$ at 5% volume fraction in 3D. However, those authors did not observe $n = 1/3$ at higher concentrations.

Our observation of $n = 1/3$ growth at critical concentration, in the "spinodal decomposition" regime where there are no nucleation barriers and where the interpenetrating domains look more like sausages than bubbles, was achieved by use of a new Monte Carlo (MC) algorithm which differs from the Kawasaki dynamics [16] generally used for such studies. This new approach slightly suppresses diffusion of material along interfaces in favor of interdomain bulk diffusion. This accelerates the approach to the asymptotic growth regime because a smaller fraction of time (real and computer) is spent on intradomain transport processes, which are suspected to generate power-law corrections to scaling [7].

Even with this acceleration, the power-law LSW growth begins only after a long transient period, the duration of which we have been able to measure as a function of annealing temperature. The transient period is strongly activated: at $T = 0.01T_c$ in 3D it lasts for $\approx 10^{112}$ MC time steps. Such times cannot be reached

by conventional MC techniques, but are easily attained using our algorithm. The ability to probe sluggish dynamics is a feature of our techniques and should make them of general interest and applicability.

We begin in Sec. II by describing our new MC technique and comparing it to conventional Kawasaki spin-exchange dynamics. In Sec. III we present results for asymptotic power-law growth. Domains are observed to grow as $t^{1/3}$ in both two dimensions (2D) and three dimensions (3D) over a wide range of annealing temperatures. In 2D, our structure factors are nearly identical to those reported by Amar *et al.* [12] for Kawasaki dynamics, and scale in a way consistent with the hypothesis that the domain patterns at different late times are statistically similar [5,15]. However, we find that our 2D structure factors differ from those reported for model B [10,11]. We also discuss two-time correlations during the ordering process, and we find that these also differ from recently reported 2D model B results [17]. Our 3D results also differ in various ways from results available for model B [11]. These results make us suspect that the asymptotic domain growth in dynamic Ising models is not described by model B. In Sec. IV we discuss phenomena that occur during the long transient period before the asymptotic growth regime.

II. MONTE CARLO KINETICS FOR THE ISING MODEL

A. Phase separation and the Ising model

We are interested in mixtures of two species of particles (atoms or molecules) which demix into two coexisting phases each rich in one of the two species. A simple model for the equilibrium statistical mechanics of this situation is the Ising model, with Hamiltonian

$$E/k_BT = -J\sum_{\langle i,j\rangle}\sigma_i\sigma_j, \tag{1}$$

where $J > 0$, the spins σ_i take on the values ± 1, and where nearest-neighbor sites $\langle i,j\rangle$ are on a regular lattice. The two spin values at each site of the Ising model represent the two types of particles. As the probability of any state in equilibrium is given by the Boltzmann distribution e^{-E/k_BT}, the ferromagnetic interaction J causes configurations where like particles are clustered together to be low in energy and therefore more likely at low temperatures.

The Ising model (in zero magnetic field, as written above) has a second-order phase transition from a disordered state at small J to an ordered state at large J. In 2D on a square lattice the phase transition occurs at $J_c = \frac{1}{2}\ln(1+\sqrt{2}) \approx 0.4407$; in 3D on a simple cubic (sc) lattice $J_c \approx 0.221\,63$; on the body centered cubic (bcc) lattice $J_c \approx 0.157\,37$; on the face centered cubic (fcc) lattice $J_c \approx 0.102\,06$ [18]. The ensemble used in equilibrium calculations is one where all spin configurations and therefore all values of total spin occur, and in zero magnetic field symmetry ensures that the average magnetization is zero. In the thermodynamic limit the equilibrium properties of this ensemble are equivalent to those of the "canonical" ensemble where only configurations with total spin zero occur.

We are interested in suitably defined *dynamics* where the total spin (i.e., the difference in volume occupied by the two components of the mixture) is fixed at zero. We suppose that at time $t = 0$ our Ising model is in equilibrium at $T = \infty$ or $J = 0$; the total spin is zero but otherwise the spins are ± 1 at random. We imagine that at $t = 0$ the temperature is quenched to a temperature $T < T_c$ ($T/T_c = J_c/J$). We then watch the spins move around for times $t > 0$. Domains form and grow in size, eventually becoming as large as the system. This is a model for the experiment where a binary mixture at critical concentration is quenched from an initial temperature well above the demixing critical temperature T_c to a final temperature below T_c.

B. Correlation function, scattering function, and domain size

The size of domains during phase separation can conveniently be obtained from measurement of two-point correlations [5]. These correlations can be directly obtained via elastic light or neutron scattering [1–3]. The two-point real-space correlation function of the spins in an Ising model is simply

$$g(\mathbf{r}) = \frac{1}{N}\sum_{\mathbf{r}'}\sigma(\mathbf{r}')\sigma(\mathbf{r}'+\mathbf{r}), \tag{2}$$

where the sum is over all N sites $\mathbf{r}'$ of the lattice, and where periodic boundary conditions are assumed.

During conserved-order-parameter domain growth $g(\mathbf{r})$ develops a distinctive oscillating-decaying shape [7]. For $\mathbf{r} = \mathbf{0}$ the correlation is unity, and decays for increasing $|\mathbf{r}|$, crossing zero and becoming negative at some distance. A sensible definition of domain size is the distance R at which this zero crossing occurs. The size R can be computed in this way either in a specific lattice direction (for the sc lattice, the 100 direction is convenient, and was used in our previous paper [14]), or for the circularly averaged $g(r)$. The length R roughly measures the average distance from the center of a domain to the surrounding domain walls and $2R$ is the mean domain diameter.

The scattering structure factor $S(\mathbf{k})$ is the Fourier transform of the correlation function $g(\mathbf{r})$:

$$S(\mathbf{k}) \equiv \frac{1}{N}\left|\sum_{\mathbf{r}} e^{i\mathbf{k}\cdot\mathbf{r}}\sigma(\mathbf{r})\right|^2. \tag{3}$$

This can then easily be averaged over directions $\hat{\mathbf{k}}$ to obtain the circularly averaged structure factor $S(k)$. The function $S(k)$ goes smoothly to zero at $k = 0$ because of the conservation law. As $k \to \infty$, $S(k) \approx k^{-(d+1)}$ because one observes scattering from the sharp interfaces, behavior often referred to as "Porod's law" [11]. Between

these limits, $S(k)$ has a peak, as one would expect for the Fourier transform of an oscillating function.

The domain size can also be computed from the first moment k^* of the circularly averaged structure factor [11,12]:

$$k^* \equiv \frac{\int_0^\infty dk\, k\, S(k)}{\int_0^\infty dk\, S(k)}. \tag{4}$$

The moment defined in this way is the characteristic spatial frequency of the domain structure, and therefore the diameter of the domains is roughly π/k^*.

C. Time autocorrelation of spins

An additional behavior that can be used to characterize domain growth is the same-site two-time autocorrelation of the spins [17,19]:

$$A(t) \equiv \sum_{\mathbf{r}} \sigma(\mathbf{r}, t_0)\sigma(\mathbf{r}, t). \tag{5}$$

This object simply tells us how likely it is for a spin to have remained in the same state from some reference time $t_0 > 0$ to time $t > t_0$.

In our notation we suppress the reference time t_0, but we must keep it in mind, as in principle the behavior of $A(t)$ could differ depending on whether t_0 is before or during the power-law scaling regime [17]. We shall focus on the case where t_0 is in the scaling growth regime since before that time the spin configuration is highly dependent on initial conditions and other nongeneric aspects of the growth process. What one expects is that for $t \gg t_0$ this correlator should decay algebraically with t. The conventional definition of the exponent is $A(t) \sim t^{-\lambda n}$.

D. Dynamical Ising models

What makes particular MC dynamics suitable for studying phase separation? The underlying physics is that of local rearrangement of the constituent particles in response to intermolecular forces, motivating MC dynamics where spins at adjacent sites are swapped at rates determined by the nearest-neighbor interactions of the spins being exchanged. The precise rules by which these nearest-neighbor spin exchanges (MC "moves" or "steps") occur define a "dynamical Ising model."

We naturally wish the equilibrium ensemble to be the well-studied Ising model Boltzmann distribution described above. This equilibrium will be obtained if the MC dynamics are ergodic, and if they satisfy detailed balance [20]. The latter condition requires the ratio of forward and reverse transition rates between each pair of states to be equal to the ratio of the Boltzmann factors for those two states. These constraints (local spin exchange moves, ergodicity, detailed balance) are very loose. Many MC rules satisfy them and without further prejudice all are equally admissible.

This arbitrariness of the dynamics is important. Some properties of the phase ordering process — e.g., the domain size growth law and the spin-spin correlation function at large distances — have been proposed to be *independent* of microscopic details of the dynamics, and to depend only on conservation laws, symmetries, and dimensionalities [5]. A large part of the aim of theory is to figure out exactly which observables are in this way "universal." The many different admissable dynamics present a useful tool for studying universality. In addition, we will show how a judicious choice of dynamics can increase the efficiency of numerical computations.

1. Kawasaki dynamics

The most commonly used exchange dynamics are due to Kawasaki [16]. At each MC step, a nearest-neighbor pair of spins are chosen at random and the change in energy ΔE that would occur if the spins were exchanged is computed. The step is then accepted with probability $\min(e^{-\Delta E/k_B T}, 1)$. The ratio of the forward and reverse processes is the desired $e^{-\Delta E/k_B T}$, ensuring detailed balance. Ergodicity is fulfilled, since one can obtain any spin state in a finite system by some sequence of steps with a nonzero probability from any other spin state.

Simulations of phase ordering following quenches to $T < T_c$ at critical concentration in 2D have been carried out by Huse [7], Amar, Sullivan, and Mountain [12], and by Roland and Grant [13], using Kawasaki dynamics. The general result obtained was that the domains grow with time as $R \sim t^{1/3}$. We will discuss these results in more detail below.

Published 3D Kawasaki simulations do not indicate that the $n = 1/3$ growth law holds near critical concentration. Instead, domains have been observed to grow very slowly, especially at low temperatures, with effective exponents well below 1/3 [15,21]. Some of our own studies of phase ordering using Kawasaki dynamics [22] for times of up to 10^6 MC steps per site (MCS) at temperatures near $0.5T_c$ were described by effective exponents $n \leq 0.2$ (see the lower two curves of Fig. 2 of Ref. [22]).

Kawasaki dynamics thus appear impractical for studies of phase separation in 3D. An explanation was suggested to us that transport of spins along domain walls, or "surface diffusion" might dominate the bulk transport of material on which the LSW scaling argument depends, at the times ($< 10^7$ MCS) accessible to Kawasaki dynamics. This idea can be made more quantitative by noting the basic rates for processes contributing to surface diffusion and to bulk diffusion. Consider a + spin at the surface of a domain wall between + and − spins, as shown in Fig. 1, that diffuses from a position A to a different position B. The Kawasaki rate for the exposed spin to slide along the interface from A to B (i.e., surface diffusion, the dotted arrow in Fig. 1) is 1, since the energy does not change during this process. If the particle detaches from the surface at A, diffuses through the domain of − spins, and reattaches at B (i.e., bulk diffusion, dashed line in Fig. 1), an energy cost of $4J$ is involved in the detachment, making bulk diffusion an activated process. Thus, in Kawasaki dynamics, bulk diffusion is suppressed by a

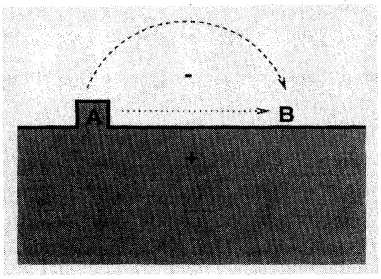

FIG. 1. Motion of single + spins contributing to surface diffusion and bulk diffusion. Dotted line: a + spin can move from A to B by surface diffusion along the interface between bulk + and − regions. Dashed line: the same + spin can move from A to B by bulk diffusion if it detaches from the interface, moves through the sea of − spins, and reattaches at B.

factor e^{-4J} relative to surface diffusion, which likely will delay the dominance of bulk transport required for LSW growth. Also, Kawasaki dynamics arbitrarily equates the basic rates for motion of spins at domain walls and in the bulk. These two facts prompted us to consider alternative spin-exchange dynamics in which the motion of spins along interfaces could be suppressed.

2. A new exchange dynamics with reduced surface diffusion

In our approach we keep track of the coordination number of each site i:

$$Q(i) = \sum_{j \in \langle i,j \rangle} \delta(\sigma_i, \sigma_j). \tag{6}$$

The $Q(i)$ run from 0 to z, where the lattice coordination number $z = 4$ for the square lattice, $z = 6$ for the sc lattice, 8 for the bcc lattice, and 12 for the fcc lattice. Isolated spins i whose neighbors are opposite in sign have $Q(i) = 0$, while spins i in the interior of domains whose neighbors all have the same sign have $Q(i) = z$. The coordination numbers provide sufficient information to compute energy changes due to spin exchanges. The change in energy resulting from an exchange of two nearest-neighbor spins i and j with opposite sign and coordination numbers $Q(i)$ and $Q(j)$ in the initial state is $\Delta E = 4J[Q(j) + Q(i) - (z-1)]$.

We order all sites into $z+1$ lists of sites with equal coordination numbers and hence with equal local environments. The number of sites in the list containing sites with coordination number q is called N_q. The rationale for this list making is simple. As phase ordering occurs (for temperatures not too close to the critical temperature) + and − spins are organized into progressively larger domains, and thus an ever-increasing fraction of the sites will have $q = z$. It is most efficient to keep track of the sites by coordination q since nontrivial exchanges involve only the continually shrinking set of sites with $q < z$.

For greater efficiency we do not use the usual accept-reject Metropolis approach with a fixed time step [20]. Instead we choose a step from the ensemble of all possible spin exchanges according to how likely it is to occur per unit time, making a time step of appropriate (variable) duration. One step of our dynamics for a 3D cubic lattice consists of (a) increment time [23] by

$$\Delta t = \left[\sum_q (1 - q/z) N_q e^{-4Jq} \right]^{-1},$$

(b) select list q with probability $P_q = \Delta t(1 - q/z)N_q e^{-4Jq}$, (c) select randomly one site i from list q, (d) select randomly a neighbor j of site i, with $\sigma_j \neq \sigma_i$, and (e) flip σ_i and σ_j, adjust the Q values of i, j, and their neighbors, and update the lists.

Ergodicity is argued to be satisfied as for other spin-exchange dynamics [20]. To prove detailed balance, let us consider a move in which a spin at site i with coordination number $Q(i)$ is selected, and exchanged with the spin at site j with coordination number $Q(j)$, one of its nearest-neighbor sites on which a spin with opposite sign is located. Let us denote the configuration before and after this move with A and B, respectively. The transition rate from configuration A to configuration B by this process is given by

$$T^{(1)}_{A\to B} = \frac{1}{\Delta t} P_{Q(i)} \frac{1}{N_{Q(i)}} \frac{1}{z - Q(i)} = \frac{1}{z} e^{-4JQ(i)} \tag{7}$$

in which the factors arise from steps (a), (b), (c), and (d), respectively. A process from state A to B could also have started with selection of site j: this process has a transition rate

$$T^{(2)}_{A\to B} = \frac{1}{z} e^{-4JQ(j)}. \tag{8}$$

The total transition rate from A to B is thus given by the sum of $T^{(1)}_{A\to B}$ and $T^{(2)}_{A\to B}$.

After this move, the spins at sites i and j have coordination numbers $(z-1) - Q(i)$ and $(z-1) - Q(j)$, and the ratio of the total transition rate for the forward and reversed process is thus given by

$$\frac{T_{A\to B}}{T_{B\to A}} = e^{-4J[Q(i)+Q(j)-(z-1)]}. \tag{9}$$

This is exactly the ratio of the Boltzmann weights of configurations A and B, and detailed balance [20] is fulfilled. Detailed balance in addition to ergodicity guarantees that equilibrium is described by the Boltzmann distribution for Hamiltonian (1). A similar Monte Carlo scheme with a varying time step can also be employed for Kawasaki dynamics by modifying steps (a) and (b) to obtain selection of neighboring sites i and j with probability proportional to $\min\left[1, e^{4J[z-1-Q(i)-Q(j)]}\right]$.

If we now compare the two processes illustrated in Fig. 1 we see that the rate for a move along the flat interface is as highly activated as detachment. Surface diffusion therefore does not dominate, in contrast with Kawasaki

dynamics. The transition rates for all moves of an isolated spin (i.e., detachment from a domain, bulk transport, and reattachment to that domain) in our dynamics are identical to those in Kawasaki dynamics, allowing the time scales of the two algorithms to be directly compared. In the LSW theory, the late-time growth is due to the dominance of bulk diffusion over all other transport processes. It is therefore reasonable that these dynamics will enter the LSW scaling regime for earlier times than Kawasaki dynamics.

III. ASYMPTOTIC POWER-LAW DOMAIN GROWTH AFTER A QUENCH

A. Method

We begin at $t = 0$ with a configuration in which an equal number of + and − spins are placed randomly on a lattice, giving a $T = \infty$ random spin state with critical concentration. Next, we apply our spin-exchange dynamics at the annealing temperature $T < T_c$ for times $t > 0$. This is standard procedure for simulation of a deep quench at $t = 0$. We are faced with the familiar conflict between our desire for large L and the finite size and speed of our computer. For our algorithm implemented on a RS6000 computer workstation we can comfortably study systems of 512^2 spins in 2D and 128^3 spins in 3D.

What one observes during a typical run is a transient period during which the domain size R is nearly stationary, followed by a power-law regime during which the domain size increases according to the LSW growth law $R \sim t^{1/3}$. When the domain diameter $2R$ approaches about 1/10 of the width of the system, finite system size effects appear, usually manifest in growth faster than $t^{1/3}$. When there are only a few domains across the system, they become increasingly correlated, accelerating the final stages of phase separation.

We are therefore limited to domain diameters smaller than about 50 in 2D, and 13 in 3D. A single run from the quench to domains which stretch 1/10 of the way across the system requires roughly 20 h of computation for the 512^2 systems, and about 12 h for the 128^3 systems (there is some quench-depth dependence to these times). Many realizations of domain growth must be averaged because for these system sizes there are strong sample-to-sample fluctuations, particularly at later times where there are a small number of domains.

B. Two dimensions

We studied the Ising model on a square lattice with $L \times L$ sites in order to compare domain growth using our dynamics with the large-scale Kawasaki-dynamics study of Amar *et al.* [12]. We examined three annealing temperatures, doing 17 runs at $T/T_c = 0.1$ and $L = 256$, five runs at $T/T_c = 0.6$ and $L = 512$, and six runs at $T/T_c = 0.01$ and $L = 512$. We also carried out 15 runs at each of $T/T_c = 0.01$ and 0.6 for 256^2 spins which gave essentially the same results as the 512^2 runs.

1. *Domain size follows LSW 1/3 law*

In Fig. 2 we show the averaged characteristic domain size $1/k^*$ determined from the first moment of the structure factor $S(k)$ [12] for the three quenches. In each case we observe power-law growth at late times with an exponent close to $n = 1/3$. At $T/T_c = 0.1$ [Fig. 2(a)], the scaling regime occurs for MC annealing times $t > 10^{12}$ or for domain diameter $\pi/k^* > 6$. At the higher temperature $T/T_c = 0.6$ [Fig. 2(b)] scaling occurs beyond about $t > 10^5$, or for $\pi/k^* > 9$. At the very low temperature $T/T_c = 0.01$ [Fig. 2(c)], we have power-law growth for $t > 10^{156}$, or for $\pi/k^* > 20$. The time for onset of power-law growth is highly activated, varying in proportion to e^{8J} for large J. A similar result was obtained for Kawasaki dynamics by Fratzl *et al.* [24], who noted that the domain sizes versus time for different quench depths could be superimposed if time was measured in units of Je^{8J}.

For $T/T_c = 0.1$, from $t = 10^{12}$ to 10^{14} the domain size follows the growth law $n = 0.355 \pm 0.004$; for $T/T_c = 0.6$, from $t = 10^5$ to $t = 10^{7.25}$ we obtain $n = 0.326 \pm 0.005$; for $T/T_c = 0.01$, from $t = 10^{155}$ to $10^{157.5}$ we obtain $n = 0.358 \pm 0.005$. The errors quoted are statistical, and do not take into account systematic errors due to finite system size. It is sensible to have slightly larger effective exponents at lower temperatures since in finite systems weaker thermal fluctuations will lead to stronger correlations that will accelerate the latest stages of simulated domain growth.

These results are in good agreement with the results of Amar *et al.*, who found, with Kawasaki dynamics after quenches to $T/T_c = 0.5$, an asymptotic growth regime beyond about $t = 10^4$ or $\pi/k^* > 6.5$ for quenches to $0.5T_c$ (see Fig. 10 of [12]; their R_1 is related to our k^* by $R_1 = 2\pi/k^*$). The exponent that they reported using 100 runs to 10^5 MCS was $n = 0.330 \pm 0.005$.

2. *Dynamical scaling of structure factor*

We have computed the scaled structure factor $(k^*)^2 S(k/k^*)$ for late times, for $T/T_c = 0.1$ [Fig. 3(a); $t = 10^{12}$ to $10^{13.5}$ with samples spaced by half decades], $T/T_c = 0.6$ [Fig. 3(b); $t = 10^{4.5}$ to 10^7 every half decade], and for $T/T_c = 0.01$ [Fig. 3(c); $t = 10^{155}$ to 10^{157} every half-decade]. In each case a collapse of the data is observed with a peak at $k/k^* \approx 0.8$, indicating dynamical scaling of the growth process. The location of the peak and the overall shape of the scaling function are the same for all quench depths, and also agree with the results of the large Kawasaki-dynamics simulation of Amar *et al.* (see Fig. 9 of Ref. [12]). This suggests that our dynamics lead to the same long-wavelength phenomena as do Kawasaki dynamics.

At each temperature there is a well-defined Porod decay [$S(k) \sim k^{-3}$] for large k which results from scattering from the randomly oriented flat interfaces. At small k, things are less clear due to our limited system sizes, but it appears that $S(k) \sim k^{2.5}$. This is consistent with the Kawasaki dynamics results of Amar *et al.*, who find

$S(k) \sim k^{2.6}$ to $k^{2.7}$ [25].

All of the late-time scaled structure factors of Fig. 3 are the same (apart from a vertical shift needed to correct for the different binodal magnetizations at different annealing temperatures). Our scaled structure factors also match those of Amar [25] for 512^2 systems at $T = 0.5T_c$ annealed for 2×10^4 and 1×10^5 Kawasaki MCS. We conclude that in 2D the scaled structure factor is independent of the annealing temperature and details of the MC dynamics.

3. *Autocorrelations in time*

Figures 2(a)–2(c) show the same-site time autocorrelation, which approaches a power-law decay $A(t) \sim t^{-\lambda n}$. Each decay represents a different initial time t_0, and of course $A(t_0) = 1$. The exponent λn depends on the choice of t_0. Yeung *et al.* [17] have argued that the autocorrelation decay depends on the statistics of the ordering field at the initial time t_0. We find evidence for this in a strong dependence of the apparent exponent λn on t_0.

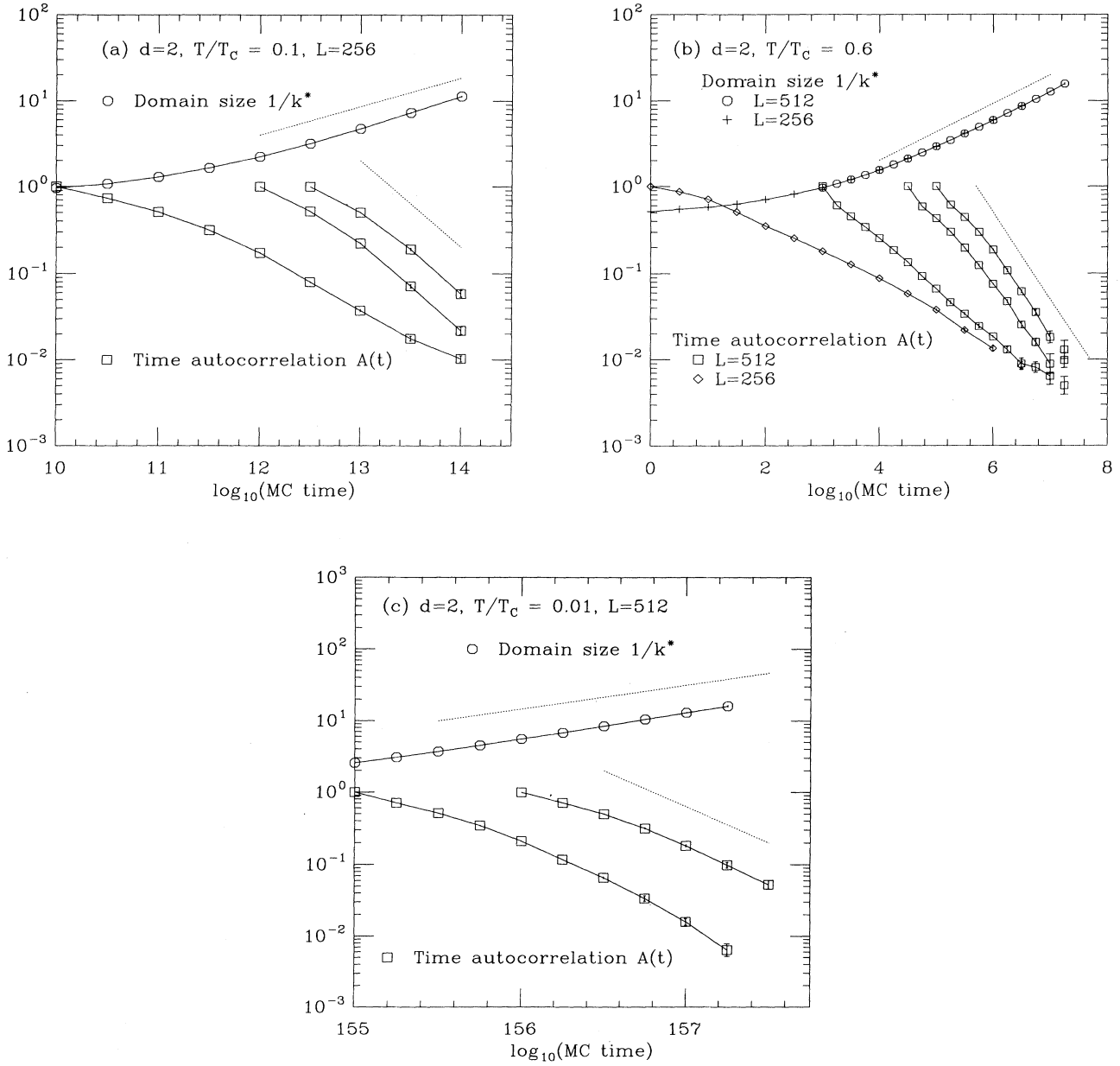

FIG. 2. Domain size and time autocorrelation in two dimensions. (a) $T/T_c = 0.1$; (b) $T/T_c = 0.6$; (c) $T/T_c = 0.01$. In each case the domain size $1/k^*$ (circles) approaches $t^{1/3}$ growth behavior (upper dashed line has a slope of 1/3). The time autocorrelations depend on the reference time t_0, but for t_0 in the scaling range the decay approaches an exponent $\lambda n = 1$ (lower dashed line has a slope of -1).

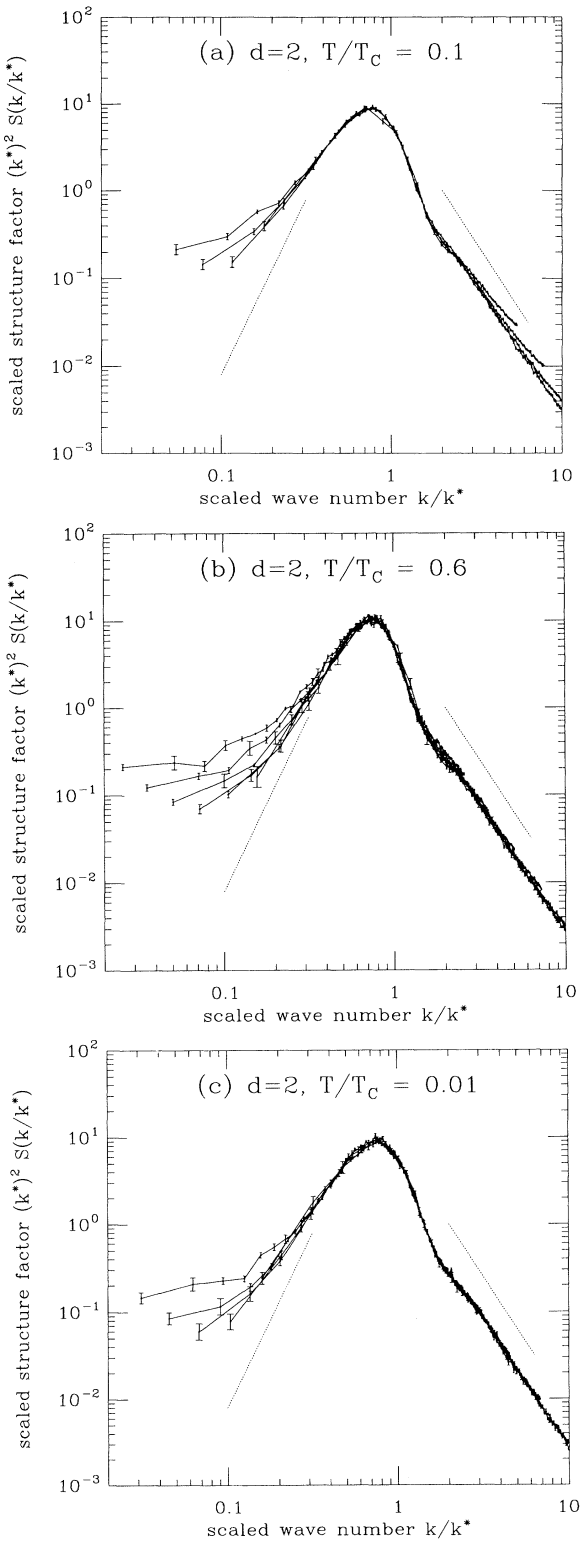

FIG. 3. Dynamical scaling of structure factor in two dimensions, in logarithmic coordinates. (a) $T/T_c = 0.1$; (b) $T/T_c = 0.6$; (c) $T/T_c = 0.01$. A k^{-3} decay characteristic of Porod scattering from the sharp domain walls occurs at large k (dashed line to right has a slope of -3); at small k, $S(k) \sim k^{2.5}$ at later times (dashed line to the left has a slope of 4).

For a 256^2 system at $T/T_c = 0.1$ [Fig. 2(a)] and for initial time $t_0 = 10^{10}$ the autocorrelation decay over the time range $t = 10^{12}$ to $10^{13.5}$ is described by the power law $\lambda n = 0.66 \pm 0.02$. Moving t_0 to later times results in an increase in this apparent exponent. For $t_0 = 10^{12}$, over the range $t = 10^{13}$ to 10^{14} we have an exponent of $\lambda n = 1.01 \pm 0.05$. For $t_0 = 10^{12.5}$, over the range $t = 10^{13.5}$ to 10^{14} we have an exponent $\lambda n = 1.0 \pm 0.1$. Thus for t_0 in the scaling regime we find an autocorrelation exponent $\lambda n \approx 1.0$. At this annealing temperature, we observed a growth exponent $n \approx 0.36$, and thus we find that $\lambda \approx 2.8$ in the scaling regime.

The same effect is observed for a 512^2 system annealed at $T/T_c = 0.6$ [Fig. 2(b)]. For $t_0 = 1$ over the time range $t = 10^5$ to $10^{6.5}$ the autocorrelation decay is described by $\lambda n = 0.43 \pm 0.04$. For $t_0 = 10^3$ the terminal power-law decay over the range from $t = 10^5$ to $t = 10^7$ is described by an exponent $\lambda n = 0.52 \pm 0.05$. For $t_0 = 10^{4.5}$ and t in the range $t = 10^6$ to 10^7 a yet higher exponent $\lambda n = 0.93 \pm 0.10$ is obtained. Use of $t_0 = 10^5$ gives a similar decay which over the range $t = 10^6$ to 10^7 has an effective exponent $\lambda n = 1.00 \pm 0.07$. For t_0 in the scaling regime $t_0 \geq 10^{4.5}$, we again find $\lambda n = 1.0$. Since $n \approx 0.33$ over this time range, we conclude that $\lambda \approx 3.0$.

In 512^2 systems at very low temperature $T/T_c = 0.01$ [Fig. 2(c)] similar autocorrelation decays are again observed for t_0 in the scaling regime. For $t_0 = 10^{155}$ we observe a decay $\lambda n = 1.45 \pm 0.25$ over the time range $t = 10^{156}$ to $10^{157.25}$. For a later $t_0 = 10^{156}$, the exponent observed over the time range $t = 10^{157}$ to $10^{157.5}$ shifts to $\lambda n = 1.10 \pm 0.15$. Again we see that $\lambda n \approx 1$ for t_0 in the scaling regime, although in this case the exponent appears to shift down to this value as t_0 is moved to later times.

In conclusion, for t_0 *in the scaling regime* where domain size $R \approx t^{1/3}$, so that the statistics at t_0 are intrinsic to the ordering process and not to some arbitrary initial condition, our 2D dynamics have $\lambda n \approx 1$, or assuming $n = 1/3$, $\lambda \approx 3$. Our results are consistent with the inequality $\lambda \geq (4 + d)/2$ recently derived by Yeung *et al.* [17] for t_0 in the scaling regime. In the same paper it is reported that $\lambda = 4$ for model B in two dimensions and t_0 in the scaling regime, which is in conflict with our result.

C. Three dimensions

In three dimensions, we previously studied [14] quenches of 64^3 spins on a sc lattice. Those runs were aimed at determining the domain size growth law. We subsequently carried out 128^3 runs in order to study the structure factor.

1. Domain growth on a 64^3 simple cubic lattice

We studied quenches from a random, critical concentration initial state to annealing temperatures $T/T_c = 0.7$, 0.5, 0.4, 0.3, 0.2, 0.15, and 0.01. Even $T/T_c = 0.7$ is quite far from the critical temperature, and the equi-

librium interface widths (thermal correlation lengths) in the final states were less than one lattice spacing in every case [18].

To measure the typical domain size R, we calculated the two-point correlation function $g(\mathbf{r},t)$ and determined its first zero crossing by solving $g(R\hat{\mathbf{x}},t)=0$, where $\hat{\mathbf{x}}$ is the 100-direction unit vector. In Fig. 4 we show $R(t)$: at each annealing temperature a transient period occurs after the quench during which $R(t)$ hardly grows, and is followed by an asymptotic regime where $R(t)$ shows power-law growth. The duration of the transient regime increases drastically as $T\to 0$. At low temperature, sharp steps in $R(t)$ occur during the transient regime: these will be discussed below.

To extract the power-law $R(t)$ exponent $n_{\rm eff}=(d\ln R/d\ln t)$ in the limit $t\to\infty$ from our simulation results, we first constructed 50 samples from each set using the bootstrap technique [26]. For each sample we carried out a least-squares fit of the $(\ln(t),\ln(R))$ data to the form $\ln(R)=n_{\rm eff}\ln(t/t_0)+\exp[-c\ln(t/t_1)]$, in the regime where $R\geq 2.0$. The second term in this function corrects for the transient behavior just before the asymptotic regime. Our results are $n_{\rm eff}=0.37(3)$, 0.35(2), 0.31(4), 0.28(2), 0.30(3), 0.33(3), and 0.32(3), for $T/T_c=0.01$, 0.15, 0.2, 0.3, 0.4, 0.5, and 0.7, respectively. These results are consistent with the exponent $n=1/3$.

The duration of the transient is due to the activated nature of bulk diffusion at late times, which follows from the energy barriers for removal of spins from domains. If we rescale the time for each simulation by the characteristic time $\tau=e^{12J}$, the asymptotic $R(t)$ curves collapse. This is illustrated in Fig. 4 by the dashed lines $R(t)=A[t/\tau]^{1/3}$, with $\tau=e^{12J}$ and $A=1.6$, which fall close to the asymptotic $R(t)$ values from the simulations, over a large range of temperatures and times. The energy scale $12J$ is the excitation energy for a spin at a corner on the sc lattice. Such sites are guaranteed on randomly oriented planar interfaces, and must be present in the domain patterns that occur at late times.

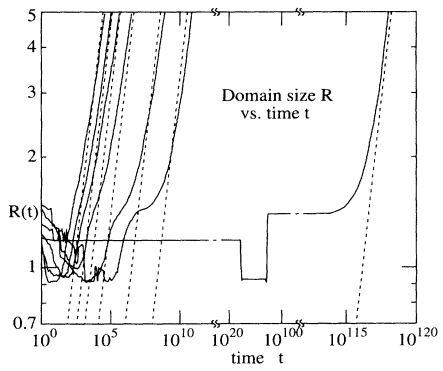

FIG. 4. Domain growth in three dimensions on a 64^3 lattice. Solid curves indicate simulation results for the domain size R as a function of time t, after a quench from $T=\infty$ to (from left to right) T/T_c =0.7, 0.5, 0.4, 0.3, 0.2, 0.15, and 0.01. The asymptotic behavior is well described by the dashed lines, which are the power laws $R(t)=A[t/\tau]^{1/3}$, with $\tau=\exp(12J)$ and $A=1.6$. As explained in the text, the unit of time is equivalent to Kawasaki spin exchanges per lattice site. Note that the (logarithmic) time scale is contracted in the range 10^{12}–10^{112} in order to show the lowest-temperature data.

2. *Domain growth on a 128^3 simple cubic lattice*

Five quenches from random, critical concentration initial states were carried out for annealing temperatures $T/T_c=0.1$ and $T/T_c=0.6$ on a 128^3 sc lattice. This system size was the minimum that allowed an estimation of the structure factor $S(k)$. From $S(k)$, the domain size $1/k^*$ was determined from its first moment k^*. The domain sizes for $T/T_c=0.1$ and 0.6 are shown in Figs. 5(a) and 5(b), respectively; in each case a growth law $1/k^*\sim t^{1/3}$ is observed at late times, in agreement with the 64^3 results.

For $T/T_c=0.1$, the domain size from $t=10^{18.5}$ to $10^{19.5}$ (at $t=10^{19.5}$ the domain diameter is $\pi/k^*\approx 15$) follows a power law with $n=0.327\pm 0.007$. At $T/T_c=0.6$, we find that from $t=10^{3.5}$ to $10^{4.5}$ (from $\pi/k^*=3.5$ to about 8) the domains grow with effective exponent $n=0.295\pm 0.002$. The latter exponent is low because we have not run to very large domains (finite size effects appear beyond these modest domain sizes), and we did not do extrapolations to determine the growth law. The effective exponents that we observe over these limited time ranges are consistent with the 64^3 lattice study, and are converging to $n=1/3$.

3. *Scaling of structure factor*

The scaled structure factor $k^{*3}S(k/k^*)$is shown in Fig. 6. At $0.1T_c$ [Fig. 6(a)] we do not observe dynamical scaling. The dashed lines show times from 10^{15} to $10^{17.5}$, during which time the domain diameter π/k^* grows from about 2.5 to 5: surprisingly, during this time window the scaled structure factor is nearly stationary even though the growth is not yet near the asymptotic regime. Then for times from $10^{17.5}$ to $10^{19.5}$ when the domain diameter grows from $\pi/k^*=5$ to 15.7 and approaches the $t^{1/3}$ growth law, we observe that dynamical scaling does not hold [solid lines of Fig. 6(a)]. The peak systematically decreases, and only the tails show a scaling collapse.

On logarithmic axes [Fig. 7(a)] we observe that for $0.1T_c$ the tails overlap quite well. We observe a clear k^{-4} Porod tail at large k expected for sharp interfaces in three dimensions. At small k, the data collapse over a larger range of k/k^* at longer times, and appear to be converging to a power law of about $k^{2.5}$, about the same small-k behavior that we observed in two dimensions.

For $0.6T_c$, the scaled structure factor is shown in Fig. 6(b) for times from 10^3 to $10^{4.5}$. Although the shape of the scaled structure factor is still evolving at these times (the whole scaled structure factor is shifting slightly to the right with time), the change in shape from $t=10^4$ to $10^{4.5}$ (rightmost two curves) is much less than

from 10^3 to $10^{3.5}$ (leftmost two curves). In logarithmic coordinates [Fig. 7(b)] the tails of the $0.6T_c$ scaled structure factors appear to be converging to a single curve at the latest times. The high-k behavior is approaching a k^{-4} Porod law behavior. From these data it is unfortunately difficult to see what the limiting small-k behavior is going to be, or to resolve details of $S(k)$ such as a small second peak at $k \approx 2k^*$ observed for model B [11].

To sum up, over the time range that we are able to observe, $S(k)$ at $0.6T_c$ appears to be converging to a form in accord with the dynamic scaling hypothesis, and has a shape roughly consistent with that observed in simulations of model B [11]. At $0.1T_c$ we see a qualitatively completely different structure factor that does not satisfy dynamical scaling at late times.

4. *Two-time autocorrelation*

Figure 5 shows the autocorrelation function $A(t)$ for 128^3 systems. At $T/T_c = 0.1$ [Fig. 5(a)] if the initial time is $t_0 = 10^{15}$ (before the scaling regime), we observe an exponent $\lambda n = 0.52 \pm 0.01$ between $t = 10^{18.5}$ and $10^{19.5}$. If t_0 is moved to the scaling regime, the expo-

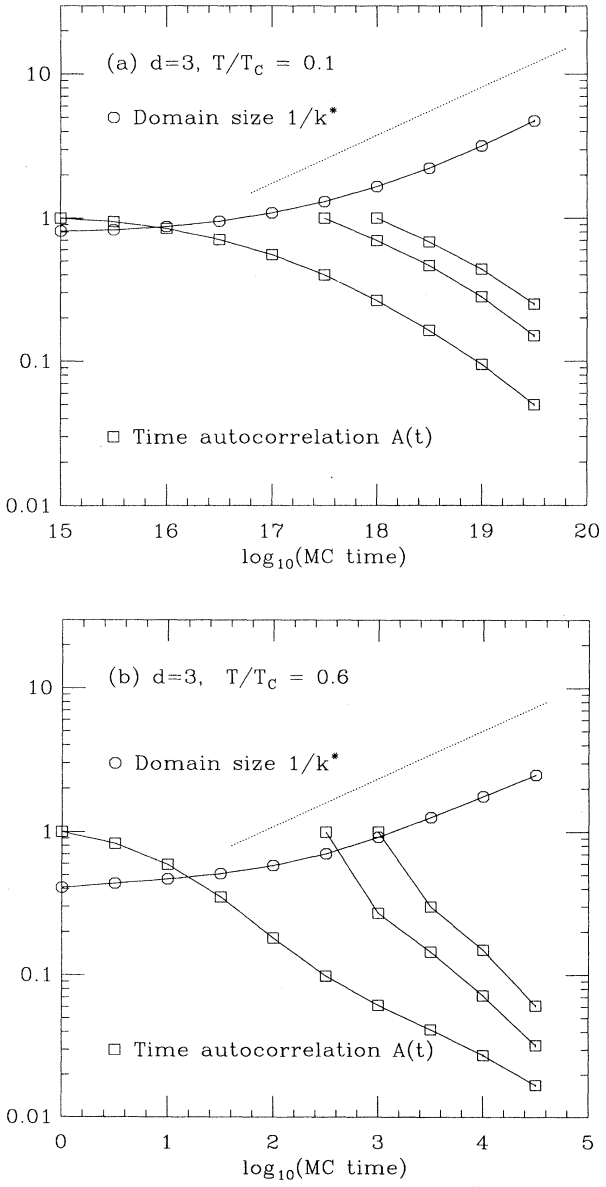

FIG. 5. Domain size and time autocorrelation for domain growth in three dimensions, on a 128^3 sc lattice, for quenches to (a) $T/T_c = 0.1$ and (b) $T/T_c = 0.6$. The size $1/k^*$ was determined from the first moment k^* of the structure factor, and grows asymptotically as $t^{1/3}$.

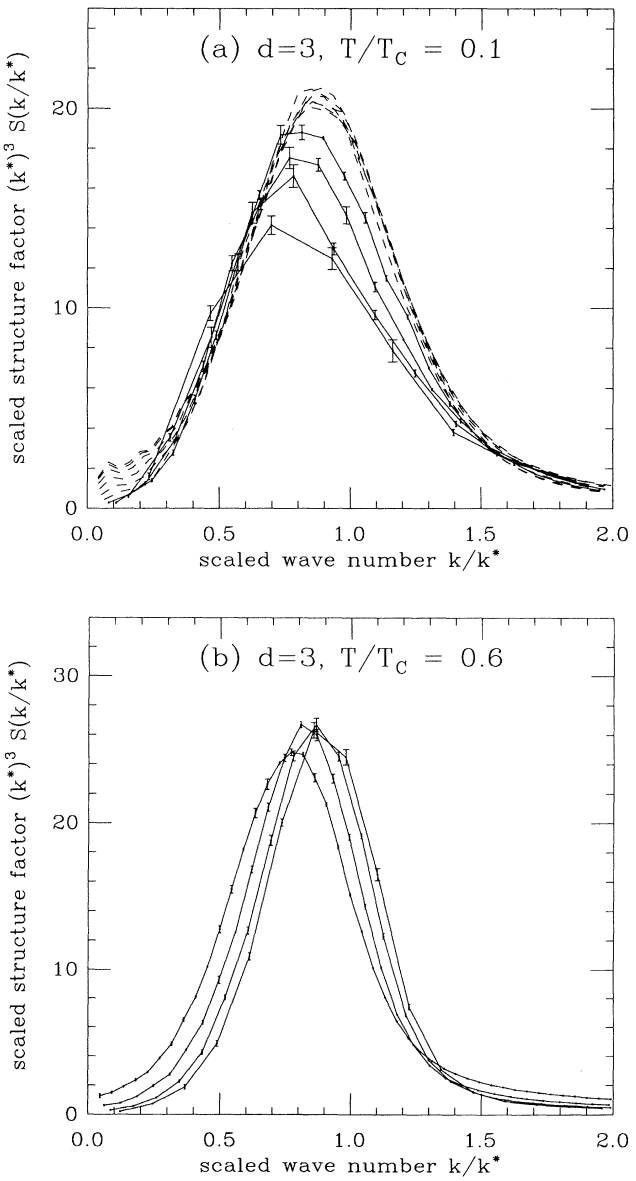

FIG. 6. Dynamical scaling for structure factor for domain growth on a 128^3 sc lattice, for quenches to (a) $T/T_c = 0.1$ and (b) $T/T_c = 0.6$.

nent observed over the time range $t = 10^{18.5}$ to $10^{19.5}$ is slightly reduced: for $t_0 = 10^{17.5}$ we find $\lambda n = 0.49 \pm 0.01$, and for $t_0 = 10^{18}$ we find $\lambda n = 0.43 \pm 0.01$. Assuming $n = 1/3$, the late time $\lambda \approx 1.5$ violates the bound $\lambda \geq (4+d)/2 = 3.5$ of Yeung, Rao, and Desai [17] by a large margin.

At $T/T_c = 0.6$ [Fig. 5(b)] we have a very limited time range from which to extract exponents. For initial time $t_0 = 1$ we observe a power-law decay with $\lambda n = 0.374 \pm 0.005$ over the time range $t = 10^{3.5}$ to $10^{4.5}$. For later t_0, faster decays are observed: for $t_0 = 10^{2.5}$, $\lambda n = 0.70 \pm 0.02$; for $t_0 = 10^3$, $\lambda n = 0.78 \pm 0.02$ over the time range $t = 10^4$ to $t = 10^{4.5}$. In the scaling regime (again assuming $n = 1/3$) we have $\lambda \approx 2.5$, which once again is a good bit below $(4+d)/2$. As in 2D, for low annealing temperatures the apparent exponent λn shifts down as t_0 is made larger; λn shifts up as t_0 is increased for higher annealing temperatures.

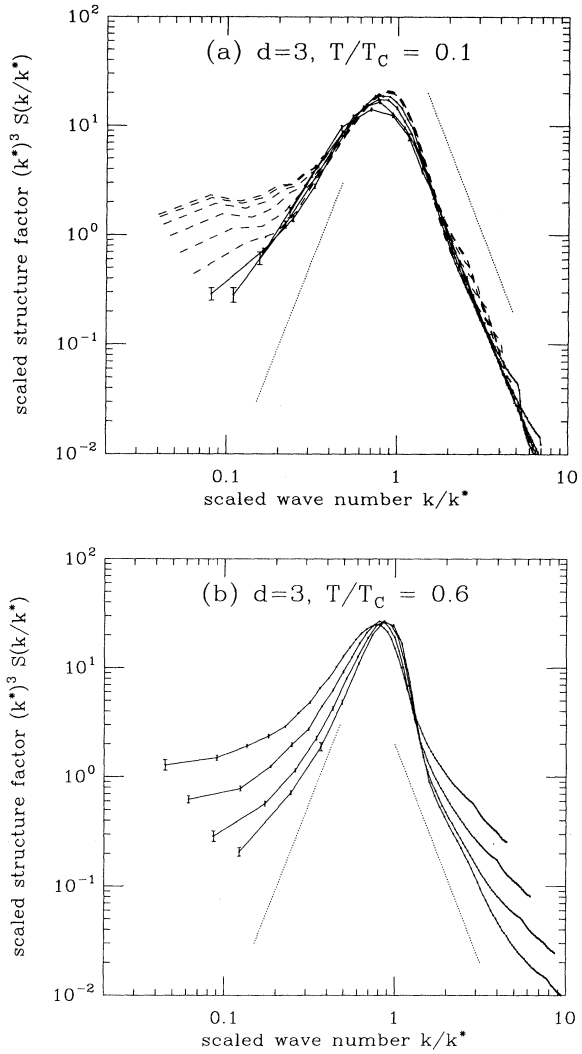

FIG. 7. Dynamical scaling for structure factor, in logarithmic coordinates, for quenches to (a) $T/T_c = 0.1$ and (b) $T/T_c = 0.6$ (dashed lines to left have slope 4; those to right have slope -4). In (a), the Porod k^{-4} behavior is clearly seen at large k; the data of (b) are consistent with this. At small k, case (a) shows $k^{2.5}$ behavior; case (b) shows a sharper k dependence. The two cases appear to be converging to different scaling functions.

IV. TRANSIENT PHENOMENA AT LOW TEMPERATURES IN THREE DIMENSIONS

In the low-temperature run ($T/T_c = 0.01$) in Fig. 4, there occurs a very long transient regime during which $R(t)$ hovers around 2. In Sec. IV B we saw that this transient has a duration of approximately e^{12J}. Closer examination of Fig. 4 reveals sharp steps in $R(t)$ for $T/T_c = 0.01$ at times e^{4J} and e^{8J}; similar steps are visible at higher temperatures. This suggests that the steps are related to the rates e^{-4Jq} for single spin exchanges involving a site of coordination number q [27].

This idea is verified by examination of the coordination number distribution N_q. Figure 8 shows N_q over the course of a 64^3 simulation on the sc lattice, following a quench to $T = 0.05T_c$. The transient behavior of the N_q may be divided into "decays," during which one of the N_q falls off over about one decade in time, and "plateaus," during which all of the N_q are essentially constant. Sharp (exponential) decays of N_0, N_1, N_2 at successively later times are clearly visible. After each decay, the time step in our simulation grows by about a factor of e^{4J}, enabling us to reach extremely large times for low temperatures. At lower temperatures, the plateaus stretch while the decays continue to require about one decade.

The basic reason for this behavior is that the moves in our dynamics for sites of coordination number q occur at rates $\sim e^{-4Jq}$. At low temperature moves of highly coordinated spins, for example $q = 3$, have very long time scales in comparison with sites with $q = 0$, 1, and 2. Thus we may ignore the dynamics of $q = 3$ sites unless the densities of $q = 0$, 1, and 2 sites are very low. But phase ordering involves an increase in the mean coordination number since equilibrated coexisting phases at low temperature will have $q \approx z$ at almost all sites.

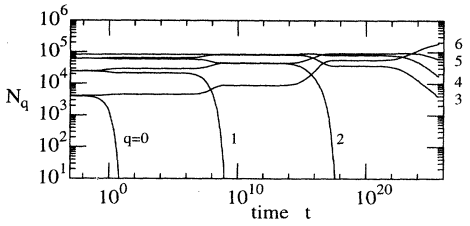

FIG. 8. Number of sites N_q with coordination number q, as a function of time after a quench from $T = \infty$ to $T = 0.05T_c$. N_0, N_1, and N_2 undergo sharp exponential decays at times of 1, e^{4J}, and e^{8J}, respectively; at a time of e^{12J} the scaling regime begins, and the remaining N_q begin to show power-law behaviors. Results are obtained from runs on a 64^3 sc lattice. As explained in the text, the unit of time is equivalent to Kawasaki spin exchanges per lattice site.

Therefore the early stages of phase separation can reasonably proceed in stages, where first (immediately after the quench) all of the energetically unfavorable $q = 0$ sites (with all neighbors of opposite sign) disappear, leaving lower-energy sites where $q \geq 1$ (sites with at least one like neighbor). Now, one has to wait a time of order $\exp(4J)$ for the $q = 1$ spins to move. Then, on that time scale the $q = 1$ spins will disappear since they will recombine to make much more stable sites where $q \geq 2$. Then nothing will happen until a time of order $\exp(8J)$ when the next characteristic time scale is reached, at which even lower-energy $q = 2$ spins can move. Iterating this reasoning, for each q we obtain a time scale $\exp(4qJ)$ characteristic to the motion of q-fold coordinated spins.

This step-by-step decay process cannot occur for all q as it is inconsistent with power-law growth. Numerically we observe that the step-by-step process is interrupted at a magic value q^* which is lattice-structure dependent. Beyond the time $\exp(4q^*J)$, the densities of all the sites begin to decay together algebraically, and the $t^{1/3}$ growth regime begins. Figure 8 shows sharp decays of the N_0, N_1, and N_2. But then power-law growth begins at $\exp(12Jq)$, and the remaining N_q for $q \geq 3$ decay as power laws of time.

For the 2D square and 3D sc lattices, we observe $q^* = 2$ and $q^* = 3$, respectively; for the bcc and fcc lattices, $q^* = 4$ and 6, respectively. These q^* values may be rationalized simply. Consider the 2D square lattice. In the scaling regime we expect the lattice to play no role in determining domain morphology. As the domains grow, the interface curvatures decay as $1/R$. Thus at the lattice scale we can think of the interfaces as nearly flat and *randomly oriented.* Random orientation implies that the number of $q = 2$ "steps" sites will be roughly as large as the number of $q = 3$ "terrace" sites in the scaling regime. Thus on the square lattice we expect $q^* = 2$, which gives the characteristic time e^{8J} for the onset of power-law growth observed by Amar, Sullivan, and Mountain [12] and by us. In 3D, q^* can be similarly rationalized by noting that arbitrarily oriented planar interfaces on the sc, bcc, and fcc lattices require $q \geq 3$, 4, and 6, respectively.

In the scaling regime on the sc lattice N_q for $q = 3, 4, 5$ approach power-law decays with exponents close to $-1/3$ in the scaling regime (Fig. 8). This can be easily understood from the scaling hypothesis, which predicts a single length R characterizing the domain size, indicating that domain walls occupy a fraction $\sim 1/R$ of the system volume [5]. For R much bigger than the lattice size and the domain wall thickness (thermal correlation length), the fractions of the domain wall regions made up of $q = 3$, 4, and 5 sites should be independent of R. Thus they should each decay as $t^{-1/3}$. If we add to this conclusion the conservation law, we see that N_6 must approach its final equilibrium value as $t^{-1/3}$.

V. CONCLUSIONS

The main result of this paper is observation of a domain growth exponent $n = 1/3$ following a quench from a disordered state, in a spin-conserving 3D dynamical Ising model. This has been done by the use of an alternative type of MC dynamics, which, compared to Kawasaki dynamics, has identical bulk diffusion and suppressed surface diffusion. We have also presented data for the 2D square-lattice dynamical Ising model. At low temperatures, transport processes are highly activated, leading to a postponement of the scaling regime to a time $\sim e^{4q^*J}$, where q^* is a number that depends on the lattice structure. On the 3D sc lattice, $q^* = 3$, and the resulting very long delay of the scaling regime at low temperatures explains why $n = 1/3$ was not previously observed in simulations of that model.

In 2D our alternative dynamics produce late-time domain growth in excellent agreement with that observed by Amar and co-workers [12,24], supporting the assumption that scaling properties of growth processes (e.g., the LSW domain growth law and the scaled structure factor) should be independent of details of the microscopic dynamics. In addition to the $t^{1/3}$ domain growth law, we find the same time scale $\exp(8J)$ for the onset of the scaling regime and essentially the same structure factor, as observed by Amar and co-workers [12,24]. The structure factor behaves according to the dynamical scaling hypothesis, satisfies Porod's law at large wave numbers, and has the same power-law behavior $[S(k) \sim k^{2.5}]$ at small wave numbers. All of these properties of the late-time growth are the same for quenches to $0.01T_c$, $0.1T_c$, and $0.6T_c$.

We also studied the same-site two-time autocorrelation function during the final power-law growth regime in 2D, and we found that it has a power-law decay with exponent $\lambda n = 1.0 \pm 0.1$. As long as both times were in the scaling regime the same exponent was observed, for all annealing temperatures and for both 256^2 and 512^2 lattices. Yeung, Rao, and Desai [17] have derived the bound $\lambda \geq (4+d)/2$: our results are consistent with this expression with the inequality changed to an equality. It would be interesting to see if the generally good agreement between our dynamics and Kawasaki dynamics could be extended to the autocorrelation exponent.

In 3D, we find $n = 1/3$ domain growth for annealing temperatures from $0.01T_c$ to $0.7T_c$. Our study of other aspects of the ordering process has led to only crude results because we were limited to lattice sizes of 128^3, and two annealing temperatures. Even so, a big difference between the structure factors at these two annealing temperatures is apparent. At $0.6T_c$, the scaled structure factor is converging to a form independent of time in accord with the dynamical scaling hypothesis. At large wave numbers, we observe Porod's law. We were unable to estimate the low-wave-number k dependence of the structure factor at $0.6T_c$.

For an annealing temperature of $0.1T_c$ we observe unexpected behavior of the structure factor. The overall shape of the stucture factor at $0.1T_c$ is very different from that at $0.6T_c$, and the tails of $S(k)$ satisfy dynamical scaling while the central peak does not. Porod's law holds in the large wave number tail while $S(k) \sim k^{2.5}$ at small wave numbers, results reminiscent of our 2D study.

These unexpected results obtained at $T = 0.1T_c$ sug-

gest further exploration on a larger, faster computer in order to see if dynamical scaling holds at later times, deeper into the scaling growth regime. But, dynamical scaling is so blatantly violated that it is difficult to see how it could be restored during the additional annealing time (a decade or so) that could reasonably be studied.

We also studied the two-time autocorrelation on the 3D sc lattice. Again we have observed a large difference between anneals at $0.6T_c$ and $0.1T_c$. At $0.6T_c$ we have found a power-law decay of the same-site autocorrelation function, and if both times are in the scaling regime we find an exponent of $\lambda n \approx 0.8$. The true exponent may be somewhat larger as we have only been able to obtain data near the beginning of the scaling regime, and a slow drift of λn to larger values with increasing t_0 is consistent with our data. At the lower annealing temperature of $0.1T_c$ in 3D we observe $\lambda n \approx 0.5$. This is quite different from the independence of λn on annealing temperature observed in 2D in the scaling regime, and deserves further study. The 3D two-time autocorrelation exponents at $0.1T_c$ strongly violate the bound $\lambda \geq (4+d)/2$ of Yeung, Rao, and Desai [17].

These qualitative differences in dynamical behavior in 3D are plausibly related to qualitative differences in equilibrium properties of the interfaces at $T = 0.1T_c$ and $T = 0.6T_c$; the equilibrium interface roughening transition is at $T_R = 0.542T_c$ [28]. During growth, equilibrium is reached on length scales comparable to the domain size R; i.e., for $T < T_R$, we can expect patches of interface of radius R to be microscopically flat and oriented (this effect is very clear in pictures of our domains). Growth for $T < T_R$ should therefore have a structure factor $S(\mathbf{k})$ which depends on direction of $\mathbf{k}$; by contrast, for $T > T_R$ we can expect $S(\mathbf{k})$ to be isotropic. Growth above and below the roughening transition should thus have different spherically averaged structure factors, and most likely different autocorrelations.

A. Dynamic Ising models vs model B

Our results suggest that there may be basic differences between domain growth in dynamical Ising models and in model B. In 2D, dynamical Ising models have scaled structure factors with $k^{*2}S(k) \approx (k/k^*)^{2.5}$ at small k, in conflict with simulations of model B in 2D at zero temperature [10] which find $k^{*2}S(k) \approx (k/k^*)^4$ at small k. Yeung has noted that at finite temperature model B should have $k^{*2}S(k) \approx (k/k^*)^2$ over a range of k/k^* which goes to zero as either of k^* or temperature go to zero. One might therefore argue that MC studies observe a fictitious effective exponent because of the crossover between the k^2 and k^4 behavior near $k = 0$. Our result that an increasing range of $(k/k^*)^{2.5}$ behavior is found at late times even at very low annealing temperatures ($0.01T_c$) argues against this interpretation.

In 2D, our dynamical Ising model has an autocorrelation exponent $\lambda \approx 3$, while for model B at zero temperature [17] $\lambda \approx 4$. Again one might argue that 512^2 2D Ising systems are not large enough and have not been run long enough to study the scaling regime. An alternative is that the scaling properties of dynamic Ising models differ from those of model B in 2D.

In 3D our dynamical Ising model results indicate that properties of late-time ($R \sim t^{1/3}$) domain growth depend on annealing temperature. At $0.6T_c$ we see a structure factor that is converging to a form satisfying dynamic scaling, as has been observed for model B [11], and in experiments on binary alloys where $t^{1/3}$ domain growth occurs [1]. At $0.1T_c$ a different structure factor and different autocorrelation exponents were observed. No similar annealing temperature effects have been observed for model B.

In the absence of an analytical theory of domain growth, we feel that we should keep an open mind about exactly what the connection is between model B and MC dynamics, and either model's relevance to experiments. This question might alternatively be addressed by (a) experimental studies of the structure factor and autocorrelation exponent in 2D for polymer films [29] or surfactant layers [30] to see if results closer to model B or dynamic Ising models are obtained; (b) theoretical studies of model B at finite temperature (most of the detailed studies of model B [10,11,17] have been done at zero temperature) to check whether some of the effects we observe might be caused by thermal fluctuations.

A final point is that our method for simulating activated kinetics should be useful for the study of a variety of problems. We have developed a related model with *enhanced* surface diffusion which is tailored to the study of equilibrium crystal shapes [31]. Our method could also be effective in studying nonequilibrium crystal shapes or other interfacial kinetics. It is straightforward to account for surface fields in order to model nonequilibrium wetting kinetics, spinodal decomposition near surfaces, and lattice-gas kinetics in porous media. Ising models have well-known equilibrium phase diagrams and are preferable to Langevin equations for these types of studies.

ACKNOWLEDGMENTS

G.B. was supported by the National Science Foundation under Grants No. ASC-93-10244 and No. DMR-9121654 through the Materials Science Center and the Cornell National Supercomputing Facility; J.M. was supported at the Center for Studies in Physics and Biology by the Meyer Foundation. We are grateful to J. Amar for giving us unpublished data. We thank G.V. Chester, M.E.J. Newman, B.W. Roberts, and J.P. Sethna for helpful comments.

[1] B.D. Gaulin, S. Spooner, and Y. Morii, Phys. Rev. Lett. **59**, 668 (1987); S. Katano and M. Iizumi, *ibid.* **52**, 835 (1984).
[2] J.S. Huang, W.I. Goldburg, and A.W. Bjerkaas, Phys. Rev. Lett. **32**, 921 (1974); Y.C. Chou and W.I. Goldburg, **20**, 2105 (1979); **23**, 858 (1981); N.C. Wong and C.M. Knobler, J. Chem. Phys. **69**, 725 (1978); **85**, 1972 (1981); Phys. Rev. A **24**, 3205 (1981).
[3] F.S. Bates and P. Wiltzius, J. Chem. Phys. **91**, 3258 (1989), and references therein.
[4] E.D. Siggia, Phys. Rev. A **20**, 595 (1979).
[5] J.D. Gunton, M. San Miguel, and P.S. Sahni, in *Phase Transitions and Critical Phenomena*, edited by C. Domb and J. Lebowitz (Academic Press, London, 1983), Vol. 8.
[6] I.M. Lifshitz and V.V. Slyozov, J. Phys. Chem. Solids **19**, 35 (1961); C. Wagner, Z. Elektrochem. **65**, 581 (1961).
[7] D.A. Huse, Phys. Rev. B **34**, 7845 (1986).
[8] R. Toral, A. Chakrabarti, and J.D. Gunton, Phys. Rev. B **39**, 4386 (1989).
[9] T.M. Rogers, K.R. Elder, and R.C. Desai, Phys. Rev. B **37**, 9638 (1988).
[10] C. Yeung, Phys. Rev. Lett. **61**, 1135 (1988).
[11] A. Shinozaki and Y. Oono, Phys. Rev. Lett. **66**, 173 (1991).
[12] J. Amar, F. Sullivan, and R. Mountain, Phys. Rev. B **37**, 196 (1988).
[13] C. Roland and M. Grant, Phys. Rev. B **39**, 11971 (1989).
[14] G.T. Barkema, J.F. Marko, and J. de Boer, Europhys. Lett. **26**, 653 (1994).
[15] J. Marro, J.L. Lebowitz, and M.H. Kalos, Phys. Rev. Lett. **43**, 282 (1979); J.L. Lebowitz, J. Marro, and M.H. Kalos, Acta. Metall. **30**, 297 (1982).
[16] K. Kawasaki, in *Phase Transitions and Critical Phenomena, Vol. 2*, edited by C. Domb and M.S. Green (Academic, London, 1972).
[17] C. Yeung, M. Rao, and R. Desai (unpublished).
[18] A.J. Liu and M.E. Fisher, Physica A **156**, 35 (1989).
[19] S.N. Majumdar, D.A. Huse, and B.D. Lubachevsky, Phys. Rev. Lett. **73**, 182 (1994).
[20] K. Binder, in *Monte Carlo Methods in Statistical Physics*, edited by K. Binder (Springer-Verlag, Berlin, 1986), Chap. 1.
[21] G.F. Mazenko, O.T. Valls, and F.C. Zhang, Phys. Rev. B **31**, 4453 (1985); G.F. Mazenko and O.T. Valls, *ibid.* **33**, 1823 (1986).
[22] G.T. Barkema and J.F. Marko, Phys. Rev. Lett. **71**, 2070 (1993).
[23] The choice of Δt in the description of our algorithm is the average time that would elapse before a change in configuration. One could alternately sample Δt from its (exponentially decaying) distribution; the spread in the absolute time after many moves would be extremely small.
[24] P. Fratzl, J.L. Lebowitz, O. Penrose, and J. Amar, Phys. Rev. B **44**, 4794 (1991).
[25] J. Amar (private communication).
[26] B. Efron and R. Tibshirani, Stat. Sci. **1**, 54 (1986).
[27] Similar steps have been observed in the total energy for an Ising model with nonconserved spin; J.D. Shore, M. Holzer, and J.P. Sethna, Phys. Rev. B **36**, 11376 (1992).
[28] K.K. Mon, D.P. Landau, and D. Stauffer, Phys. Rev. B **42**, 545 (1990).
[29] P. Bassereau, D. Brodbreck, T.P. Russell, H.R. Brown, and K.R. Shull, Phys. Rev. Lett. **71**, 1716 (1993); G. Krausch (private communication).
[30] M. Seul, N.Y. Morgan, and C. Sire, Phys. Rev. Lett. **73**, 2284 (1994).
[31] G.T. Barkema, M.E.J. Newman, and M. Breeman, Phys. Rev. B **50**, 7946 (1994).

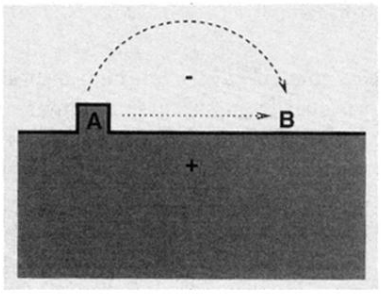

FIG. 1. Motion of single + spins contributing to surface diffusion and bulk diffusion. Dotted line: a + spin can move from A to B by surface diffusion along the interface between bulk + and − regions. Dashed line: the same + spin can move from A to B by bulk diffusion if it detaches from the interface, moves through the sea of − spins, and reattaches at B.